Table I. Antibonding Contributions of the Oxygen p Orbitals of Mo–O–Mo Bridges in the t_{2g} Block Band Orbitals of the Mo_2O_9 Layer[a]

band orbital	wave vector	unit cell orbital	intrachain: within a unit cell	intrachain: between nearest-neighbor unit cells	interchain
13a	Γ	ϕ_1^-	N	N	N
13b	Γ	ϕ_1^+	Y	Y	N
14a	M	ϕ_1^-	N	N	N
14b	M	ϕ_1^+	Y	Y	N
16a	Γ	ϕ_2^+	N	N	N
16b	Γ	ϕ_2^-	Y	Y	N
17a	K′	ϕ_2^+	Y	Y	N
17b	K′	ϕ_2^-	N	N	N
20a	Γ	ϕ_3^-	N	N	N
20b	Γ	ϕ_3^+	y	y	Y
21a	M	ϕ_3^-	N	N	Y
21b	M	ϕ_3^+	y	y	N

[a] The presence of the antibonding contribution is indicated by the symbols Y or y, and the absence of it by the symbol N. The symbols Y and y refer to the stronger and the weaker antibonding contributions discussed in connection with **9** and **10**.

indicated by the symbols Y and y, respectively. **20a** has no oxygen p-orbital contribution from the Mo–O–Mo bridges and thus has the same energy as **13a**. **20b** has oxygen p-orbital contribution from all the intra- and interchain Mo–O–Mo bridges, unlike **13b**, which has oxygen p-orbital contribution only from the intrachain Mo–O–Mo bridges. Nevertheless, **20b** is degenerate with **13b** since the sum of two weak antibonding p-orbital contributions per unit cell is equivalent to one strong antibonding p-orbital contribution per unit cell. **21a** has one strong antibonding p-orbital contribution per unit cell, while **21b** has two weak antibonding p-orbital contributions per unit cell. Consequently, **21a** and **21b** are nearly degenerate, and their energies lie at the midpoint between **20a** and **20b**. This explains why bands c and d are dispersive along Γ → M and why their dispersion is half as strong as that of bands a and b along Γ → K′. In a similar way, the Mo_2O_9 layer **7c** can also be employed to show that bands c and d are equally dispersive along Γ → K′, and their dispersion is half as strong as that of bands a and b along Γ → K′.

Concluding Remarks

Our tight-binding band calculations performed on a single Mo_6O_{17} layer show the presence of three partially filled d-block bands. In agreement with the Zachariasen analysis,[7] those bands are essentially derived from the t_{2g} levels of the MoO_6 octahedra belonging to the innermost two sublayers of Mo_6O_{17}. Between adjacent Mo_6O_{17} layers, therefore, there is practically no overlap as far as the partially filled d-block bands are concerned. Thus our conclusions based upon a single Mo_6O_{17} layer are valid in discussing the electronic properties of $K_{0.9}Mo_6O_{17}$, as supported by the excellent agreement with experiment: The Fermi surfaces of the three partially filled bands show that $K_{0.9}Mo_6O_{17}$ is a 2D metal, its CDW at 120 K results from the nesting of one of the three Fermi surfaces, and the remaining two provide electron and hole carriers below 120 K. These conclusions are also valid for $Na_{0.9}Mo_6O_{17}$ and $TlMo_6O_{17}$, which are isostructural with $K_{0.9}Mo_6O_{17}$. However, we note that the sizes of the hole and electron pockets of the first and third Fermi surfaces (Figures 5a,c, respectively) are not so small (about $^1/_{18}$ and $^1/_6$ of the Brillouin zone, respectively) as suggested by the Shubnikov–de Haas study[2d] on $K_{0.9}Mo_6O_{17}$. A further experimental study is necessary. Finally, our orbital interaction analysis for the t_{2g}-block bands of the innermost two sublayers of Mo_6O_{17} shows that their essential dispersion characteristics are simply governed by whether or not the orbitals of bridging oxygen atoms can mix with the molybdenum t_{2g} orbitals.

Acknowledgment. This work was supported by NATO, Scientific Affairs Division, and also by DOE, Office of Basic Sciences, Division of Materials Sciences, under Grant DE-FG05-86-ER45259. We express our appreciation for computing time on the ER-Cray X-MP computer, made available by the DOE. We thank E. Benvas and C. Escribe-Filippini for helpful previous speculations on the Fermi surface of $K_{0.9}Mo_6O_{17}$, and Prof. M. Greenblatt for reprints and preprints.

The Variable-Temperature ESR Characterization of the Fluxional d^9 Complex Bis(1,2-bis(diphenylphosphino)ethane)rhodium(0), $Rh(dppe)_2^0$

Karl T. Mueller, Amanda J. Kunin, Stephen Greiner, Thomas Henderson, Robert W. Kreilick,* and Richard Eisenberg*

Contribution from the Department of Chemistry, University of Rochester, Rochester, New York 14627. *Received February 2, 1987*

Abstract: A variable-temperature ESR study of the paramagnetic complex $Rh(dppe)_2^0$ has been performed. The complex is found to be fluxional on the ESR time scale. At 270 K the ESR spectrum of the complex in toluene consists of a symmetric five-line pattern with $\langle A \rangle_P$ of 52 G. Upon cooling, an alternating line width effect is seen, and the spectrum changes to a pattern showing coupling to two different pairs of P donors with hyperfine couplings of 37.5 and 65 G. Analysis of the dynamic behavior leads to activation parameters $\Delta H^\ddagger$ and $\Delta S^\ddagger$ of 3.54 kcal/mol and −4.6 cal/(mol K), respectively, for the exchange process. Possible mechanisms for the exchange are pairwise lengthening and shortening of the Rh–P bonds and angular distortion of the complex to a species of C_2 symmetry. A bimolecular equilibrium is also observed by a significant decrease in the intensity of the ESR signal as the temperature is lowered. The ΔH and ΔS values for this equilibrium are −13.4 kcal/mol and −49.8 cal/(mol K), respectively, consistent with either a dimerization or the formation of an intimate ion pair, $[Rh(dppe)_2]^+[Rh(dppe)_2]^-$, for this sterically crowded system. The complex $Rh(dppe)_2^0$ is also found to react with H_2 at room temperature to form the known hydride complex $RhH(dppe)_2$.

The fluxionality of inorganic and organometallic compounds has been vigorously studied during the last two decades.[1] In general, this type of dynamic behavior in solution has been followed by variable-temperature NMR investigation from which rate

0002-7863/87/1509-6313$01.50/0

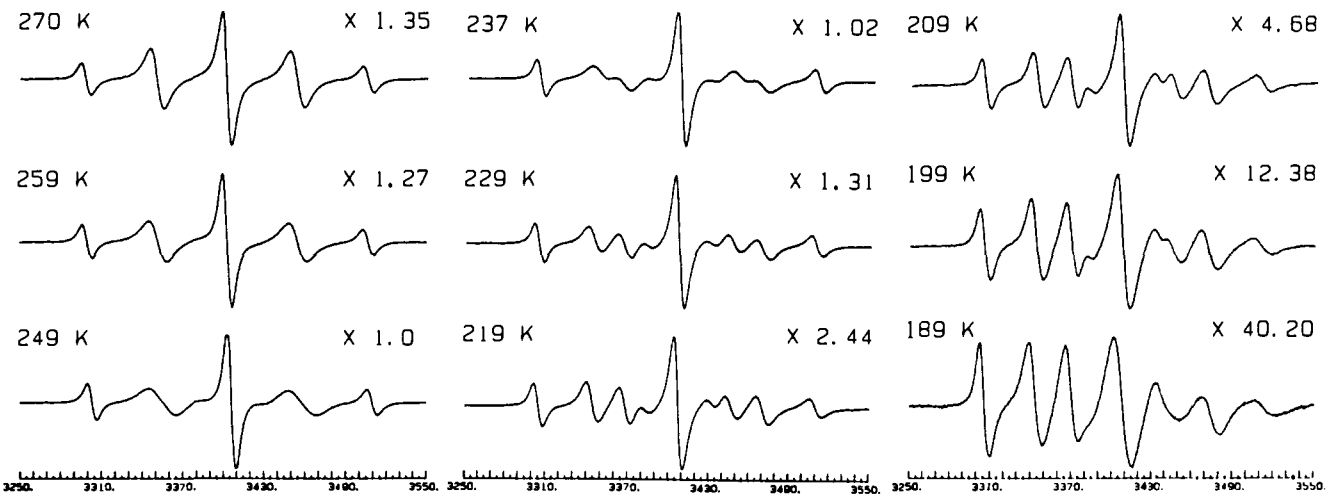

Figure 1. Variable-temperature ESR spectra of $Rh(dppe)_2^0$ in toluene. A scale factor is shown at the right of each spectrum to normalize for the most intense signal seen at 249 K.

constants for exchange at different temperatures and activation parameters for the exchange process are determined. By this method, fluxional processes as rapid as ca. 10^6 s^{-1} have been examined.

By contrast, the study of fluxionality of paramagnetic inorganic and organometallic compounds by variable-temperature ESR spectroscopy has been pursued in only a very few cases. In the first of these,[2] Krusic examined a series of (η^3-cycloalkenyl)Fe-$(P(OMe)_3)_3$ complexes in which the phosphite ligands exchanged environments. Two processes were observed with rates of 2×10^8 and 10^{10} s^{-1} at room temperature. Because ESR transitions are of higher energy than NMR transitions, the "time scale" of ESR is shorter than that of NMR, allowing the direct observation of more rapid processes when they occur in appropriate paramagnetic systems. In 1984, Rieger and co-workers examined a series of d^9 Co complexes of formula $(\eta^2$-RCCR)$Co(CO)_xL_{3-x}$, where L is tertiary phosphine, phosphite, or arsine, and concluded that the ligands L were exchanging environments at rates of $\sim 5 \times 10^{10}$ s^{-1} based on ESR line widths at different temperatures.[3]

Baker and Krusic[4] have recently analyzed the fluxional behavior of the 33 e^- and 35 e^- species $Fe_2(CO)_x(\mu$-$PR_2)$, where $x = 7, 8$. A related series of radicals, $Fe_3(CO)_{9-x}L_x(\mu_3$-$PPh)_2^-$, has been studied by Ohst and Kochi, who show that the clusters rearrange rapidly although their fluxionality is not observed directly by variable-temperature ESR spectroscopy.[5] For coordination complexes, the existence of fluxionality on the ESR time scale has been inferred by changes in **g** tensor anisotropy in rigid media as a function of temperature, as has been reported for $[Cu(phen)_2(OAc)]^+$ and related systems.[6]

Recently we reported the chemical reduction of the cationic, square-planar complex $Rh(dppe)_2^+$ with a description of the spectroscopic and chemical characterization of the 1 e^- reduction product $Rh(dppe)_2^0$.[7] One aspect of this characterization was particularly noteworthy and merited further study. Specifically, the ESR spectrum of this d^9 species showed a temperature dependence which indicated that $Rh(dppe)_2^0$ was (a) fluxional on the ESR time scale and (b) participating in an observable bimolecular equilibrium. In this paper, we describe a more detailed study of the temperature-dependent ESR spectrum of $Rh(dppe)_2^0$ together with an analysis of its fluxionality and the bimolecular equilibrium in which it participates. Additionally, we describe an interesting reaction that $Rh(dppe)_2^0$ undergoes with molecular hydrogen.

ESR Studies of Rh(0) complexes are relatively few in number, and particular systems whose ESR spectra have been reported include RhL_2 (L = 2,2′-bipyridine, 1,10-*o*-phenanthroline),[8] RhL(diolefin) (diolefin = 1,5-cyclooctadiene, norbornadiene),[9] $Rh(PPh_3)_4$,[10] $Rh(CO)(PPh_3)_3$,[11] and $Rh(P(OPh)_3)_4$.[12] The most detailed analysis of a Rh(0) ESR spectrum has been provided by George et al.[12] for the tetrakis phosphite system $Rh(P(OPh)_3)_4$. These investigators find ligand hyperfine coupling to four equivalent ^{31}P nuclei and essentially no coupling to ^{103}Rh. In frozen glass a near axial **g** tensor is observed, which together with the equivalence of the ligand hyperfine coupling, is used to assign a D_{2d} distorted tetrahedral structure to this d^9 species. The absence of ^{103}Rh hyperfine coupling is also noted in the ESR spectra of other Rh(0) systems.[8-11] None of these Rh(0) systems was reported to exhibit temperature-dependent behavior indicative of stereochemical nonrigidity in solution.

Results and Discussion

The ESR spectrum of $Rh(dppe)_2^0$ in toluene solution was recorded from 270 to 189 K as shown in Figure 1. At the high-temperature limit, the intensely blue solution shows a symmetric 5-line pattern with $\langle g \rangle = 2.027$, $\langle A \rangle = 52$ G, and binomial intensities (1:4:6:4:1) indicative of hyperfine coupling to four equivalent P nuclei. The five lines correspond to the transitions for $M = 2, 1, 0, -1, -2$, where $M = \sum m_I$ with m_I being the nuclear spin quantum number for each P. There is no observable coupling

(1) Jackman, L. M.; Cotton, F. A., Eds. *Dynamic* Nuclear Magnetic *Resonance Spectroscopy*; Academic: New York, 1975 and references therein. Other recent references may be found in the following: (a) Cotton, F. A.; Wilkinson, G. *Advanced Inorganic Chemistry*, 4th ed.; Wiley-Interscience: New York, 1980; pp 1217–1233. (b) Atwood, J. D. *Inorganic and Organometallic Reaction Mechanisms*; Brooks/Cole Publishing: Monterey, CA, 1985; Chapter 7. (c) Lukehart, C. M. *Fundamental Transition Metal Organometallic Chemistry*; Brooks/Cole Publishing: Monterey, CA, 1985; Chapter 7. (d) Douglas, B.; McDaniel, D. H.; Alexander, J. J. *Concepts and Models of Inorganic Chemistry*, 2nd ed.; John Wiley and Sons: New York, 1983; pp 322, 696–704.

(2) Ittel, S. D.; Krusic, P. J.; Meakin, P. *J. Am. Chem. Soc.* **1978**, *100*, 3264.

(3) Casagrande, L. V.; Chen, T.; Rieger, P. H.; Robinson, B. H.; Simpson, J.; Visco, S. J. *Inorg. Chem.* **1984**, *23*, 2019.

(4) Baker, R. T.; Krusic, P. J.; Calabrese, J. C.; Roe, C. D. *Organometallics* **1986**, *5*, 1506. Baker and Krusic have also seen fluxional behavior for the Ti(III) radical $(C_5Me_5)Ti(PCy_2)_2(PMe_3)$, which will be reported shortly. Baker, R. T., personal communication.

(5) Ohst, H. H.; Kochi, J. K. *J. Am. Chem. Soc.* **1986**, *108*, 2897.

(6) (a) Clifford, F.; Counihan, E.; Fitzgerald, W.; Seff, K.; Simmons, C.; Tyagi, S.; Hathaway, B. *J. Chem. Soc., Chem. Commun.* **1982**, 196. (b) Fitzgerald, W.; Hathaway, B.; Simmons, C. J. *J. Chem. Soc., Dalton Trans.* **1985**, 141 and references therein.

(7) Kunin, A. J.; Nanni, E. J.; Eisenberg, R. *Inorg. Chem.* **1985**, *24*, 1852.

(8) Caldaru, H.; DeArmond, M. K.; Hanck, K. W.; Sahini, V. E. *J. Am. Chem. Soc.* **1976**, *98*, 4455.

(9) Fordyce, W. A.; Pool, K. H.; Crosby, G. A. *Inorg. Chem.* **1982**, *21*, 1027.

(10) Olson, D. C.; Keim, W. *Inorg. Chem.* **1969**, *8*, 2028.

(11) Zotti, G.; Zecchin, S.; Pilloni, G. *J. Electroanal. Chem.* **1984**, *175*, 241. Zotti, G.; Zecchin, S.; Pilloni, G. *J. Organomet. Chem.* **1983**, 246, *61*.

(12) George, G. N.; Klein, S. I.; Nixon, J. F. *Chem. Phys. Lett.* **1984**, *108*, 627. Nixon, J. F., personal communication.

Table I. Rate Constants for Interchange of P Nuclei in $Rh(dppe)_2^0$

temp, (K)	10^{-7} k_{ex} (s^{-1})	temp, (K)	10^{-7} k_{ex} (s^{-1})
270	100	219	12.5
259	50	209	10.0
249	33	199	5.0
237	27	189	3.3
229	16.4		

to ^{103}Rh which is consistent with previous reports of Rh(0) ESR spectra. As the temperature is lowered, three distinct phenomena are observed to occur. First, within the range 270–189 K, an alternating line width effect is seen, revealing the fluxional behavior of $Rh(dppe)_2^0$. Second, below 249 K, the integrated intensity of the ESR signal decreases with decreasing temperature because of a bimolecular reaction involving two $Rh(dppe)_2^0$. Third, anisotropic broadening of the lines is observed due to slowed molecular tumbling at lower temperatures. Each of these spectral features will be analyzed to yield information about the $Rh(dppe)_2^0$ system.

Alternating Line Width Effect. As the temperature is lowered from 270 K, the symmetric 5-line ESR pattern exhibits striking changes as shown in Figure 1. Specifically, within the range 270–189 K the transitions corresponding to M values of +1 and −1 each broaden and separate into two distinct lines. In addition, two of the six components of the central line with $M = 0$ also broaden and split into separate lines so that at the low-temperature limit the spectrum is readily interpretable in terms of two different ^{31}P hyperfine couplings of 37.5 and 65 G. The observed change between the limiting spectra at 270 and 189 K is a classic example of the alternating line width effect and shows $Rh(dppe)_2^0$ to be fluxional on the ESR time scale.

The alternating line width effect has been noted in the chemical literature since 1962,[13-15] and a number of systems, primarily of organic radical anions, have been found which exhibit this type of spectral variation.[16] The effect arises because of intra- or intermolecular interchange which occurs at a frequency similar to the difference in hyperfine coupling constants of the exchanging nuclei. While the alternating line width effect has been seen in the ESR spectra of organometallic radicals, the present study is the first to observe this effect with a simple transition-metal complex having only one type of donor ligand.

The exchange process for $Rh(dppe)_2^0$ which leads to the observed spectral changes as a function of temperature is that of the two-jump model involving two sets of two *completely* equivalent phosphorus nuclei. The term equivalence denotes that the hyperfine splittings are equal when averaged over time, whereas complete equivalence means that two nuclei have the same hyperfine splittings at any instant. The theory proposes that the two sets of completely equivalent P atoms undergo interchange with anti-correlated hyperfine splittings such that the sum of the two splittings remains a constant as one splitting increases and the other decreases.[16a] The rate of the interchange is of the order of the difference in the P hyperfine coupling constants.

In order to analyze the ESR spectra of Figure 1, we have used a modified form of a computer program written by Bolton and Sullivan[16] for the alternating line width effect. The program as published assumes a four-jump model but can be applied to the present system in which two sets of two completely equivalent nuclei are averaged. The program calculates the ESR line shape for a given set of spectral parameters and a rate constant for interchange. Through adjustment of these parameters and the interchange rate constants, satisfactory fits between observed and calculated spectra were obtained as judged by visual comparison. In Table I, the rate constants for exchange determined in this way are presented, and in Figure 2, representative simulated and experimental spectra are shown.

The results of Table I can be used to obtain activation parameters based on the Eyring equation (eq 1), where k_{ex} is the rate constant for exchange of the two sets of P atoms, k_B is the Boltzmann constant, and h is Planck's constant. A plot of ln

$$\ln (k_{ex}/T) = \ln (k_B/h) - \Delta H^{\ddagger}/RT + \Delta S^{\ddagger}/R \qquad (1)$$

(k_{ex}/T) vs. $1/T$, shown as Figure 3, yields an enthalpy of activation, $\Delta H^{\ddagger}$, for the interconversion of 3.54 kcal/mol and an entropy of activation, $\Delta S^{\ddagger}$, of −4.6 cal/(mol·K).

The fluxionality observed is attributed to stereochemical nonrigidity of the $Rh(dppe)_2^0$ molecule in solution. While the static structure of this d^9 complex is unknown, reasonable initial guesses regarding its coordination geometry include a square plane, a tetrahedron, and a structure distorted between these two limits having D_{2d} symmetry for the P donors. None of these structures, however, distinguishes the P nuclei into two sets. Likewise, any angular motion between these structures, if constrained to follow the common symmetry (D_{2d}), will not differentiate the four equivalent P donors. We therefore propose two distortions of the complex which can lead to the desired result. In the first, the two hyperfine coupling constants that the complex exhibits at low temperature arise from two sets of Rh–P distances. During exchange, the Rh–P distances change in a correlated way with the longer Rh–P distances shortening and the shorter ones lengthening as shown in eq 2. It is not possible to discern from the data what the spatial orientation of the P donor atoms is (i.e., what the coordination geometry is), or indeed whether the two completely equivalent phosphorus atoms are on the same bis(diphenylphosphino)ethane ligand. While the motion of eq 2 is similar to one of the normal modes of a four-coordinate complex, it is clear from the rate constants of Table I that the observed process extends well beyond the vibrational time scale and must therefore involve Rh–P displacements of greater magnitude than is found for Rh–P stretches.

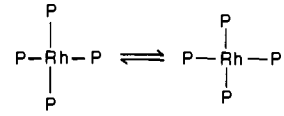

(2)

In the second possible rearrangement mechanism, differentiation of the P donors is achieved by angular distortion alone and requires a reformulation of the electronic structure of $Rh(dppe)_2^0$. If the half-occupied molecular orbital in this odd-electron species is presumed to exert a normal stereochemical influence, then the 17 e^- species may adopt a structure distorted toward a trigonal bipyramid with two axial and two equatorial P donors. Interconversion can then occur via pseudorotation as in eq 3.

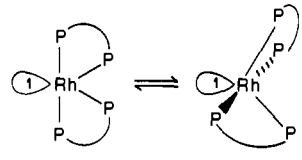

(3)

Bimolecular Equilibrium. The intensity of an ESR signal that follows normal Curie law behavior should increase as the temperature decreases since the paramagnetic susceptibility is inversely proportional to the absolute temperature of a sample. Therefore, a decline in intensity of the ESR signal with decreasing temperature indicates the disappearance of the paramagnetic species, possibly via dimerization, disproportionation, or reaction to form a diamagnetic product.

We observe a distinct drop in intensity in the spectra of the $Rh(dppe)_2$ system as the temperature is lowered below 249 K. As reported previously by us,[7] the color of the solution in toluene also changes from blue to red-brown as the temperature is decreased. These observations, which are reversible, strongly suggest a temperature-dependent equilibrium in which two paramagnetic

(13) Freed, J. H.; Fraenkel, G. K. *J. Chem. Phys.* **1962**, *37*, 1156.
(14) Bolton, J. R.; Carrington, A. *Mol. Phys.* **1962**, *5*, 161.
(15) Freed, J. H.; Bernal, I.; Fraenkel, G. K. *Bull. Am. Phys. Soc.* **1962**, *7*, 42.
(16) (a) Sullivan, P. D.; Bolton, J. R. *Adv. Magn. Reson.* **1970**, *4*, 39 and references therein. (b) Wertz, J. E.; Bolton, J. R. *Electron Spin Resonance: Elementary Theory and Practical Applications*; McGraw-Hill: New York, 1972; Chapter 9.

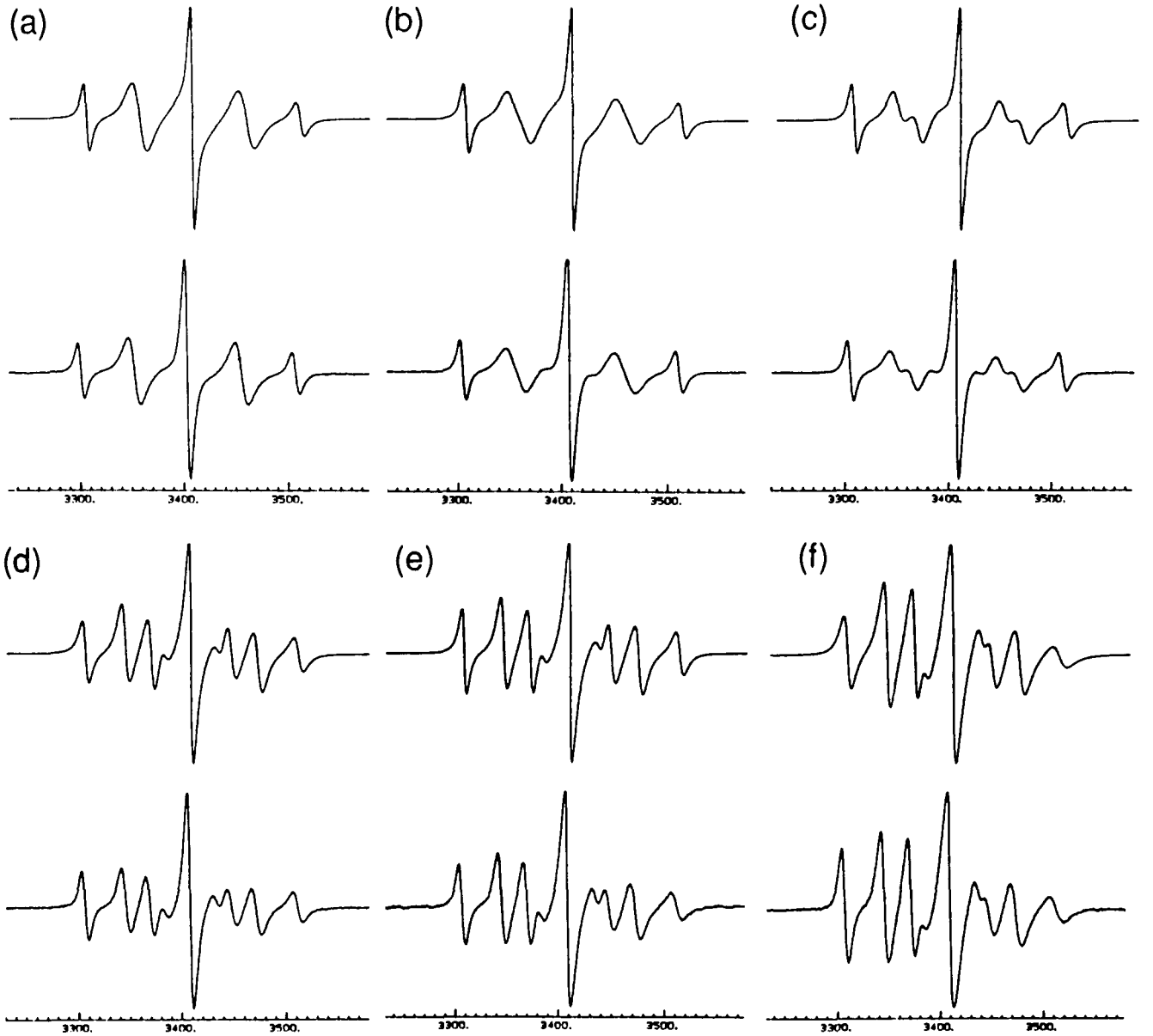

Figure 2. Calculated (top) and experimental ESR spectra for $Rh(dppe)_2^0$ at different temperatures: (a) 259 K; (b) 249 K; (c) 237 K; (d) 219 K; (e) 209 K; (f) 199 K.

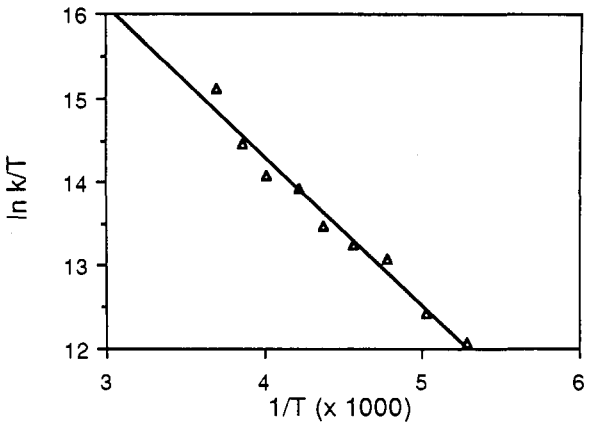

Figure 3. Eyring plot for the fluxional process involving $Rh(dppe)_2^0$.

$Rh(dppe)_2^0$ molecules interact to form a diamagnetic dimer or an ion pair, eq 4 and 5, respectively.

$$2Rh(dppe)_2^0 \rightleftharpoons Rh_2(dppe)_4 \quad (4)$$

$$2Rh(dppe)_2^0 \rightleftharpoons [Rh(dppe)_2]^+[Rh(dppe)_2]^- \quad (5)$$

From the integrated intensity of the ESR absorption spectrum at different temperatures, it is possible to calculate the equilibrium constant for (4) or (5) as a function of temperature and obtain thermodynamic parameters for this process. At 249 K and above, the ESR signal follows normal Curie behavior, and it is assumed that all $Rh(dppe)_2$ species in solution exist as 4-coordinate paramagnetic monomers. Below 249 K, the ESR signal intensity decreases with decreasing temperature. The equilibrium constant expression for (4) is shown as eq 6, where C_0 represents the total concentration of $Rh(dppe)_2$ species in solution and α is the fraction of $Rh(dppe)_2$ species existing as paramagnetic monomer. A completely analogous equation can be written for equilibrium 5. The fraction corresponding to the dimer in eq 6 is obtained through a material balance expression.

$$K = \frac{1}{2C_0}\left[\frac{(1-\alpha)}{\alpha^2}\right] \quad (6)$$

If the observed ESR intensity at temperature T is represented by I^T, then the intensity that should be seen at temperature T if $Rh(dppe)_2^0$ follows Curie behavior, $I_0{}^T$, is given by eq 7, and the fraction α is given by eq 8. By substitution, the equilibrium

$$I_0^T = I^{249}\left(\frac{249}{T\,\mathrm{K}}\right) \quad (7)$$

$$\alpha = \frac{I^T}{I^{249}(249/T)} \quad (8)$$

constant expression (eq 6) can be written in terms of the observed ESR intensities as eq 9.

$$K = \frac{I^{249}(I_0^T - I^T)}{2C_0(T/249)(I^T)^2} \quad (9)$$

Table II presents a tabulation of the observed ESR intensities as a function of temperature and the calculated equilibrium constants based on these data and an initial concentration of ca. 4 mM. Using the data of Table II, we construct a plot of ln K vs. $1/T$ shown as Figure 4 to obtain ΔH of −13.4 kcal/mol and ΔS of −49.8 cal/(mol·K) for the equilibrium between Rh(dppe)$_2^0$ and either the dimer species $Rh_2(dppe)_4$ or the intimate ion pair $[Rh(dppe)_2]^+Rh(dppe)_2]^-$. The entropy value is quite negative, consistent with either of the two possible equilibria (eq 4 and 5) involving a sterically crowded system.

While the ESR intensity data as a function of temperature do not allow us to distinguish which equilibrium (eq 4 or 5) is operative, this question has been addressed by us previously.[7] Whereas the blue solution of Rh(dppe)$_2^0$ is inert to MeOH at 298 °K, the red-brown solution at 230 K reacts with 1–5 equiv of MeOH over a period of 2–3 h to form RhH(dppe)$_2$ and Rh(dppe)$_2^+$. Since a solution of Rh(dppe)$_2^-$ prepared independently reacts with a comparable amount of MeOH over a 1-h period to form RhH(dppe)$_2$, we conclude that the low-temperature solution of Rh(dppe)$_2^0$ contains significant amounts of Rh(dppe)$_2^-$. Thus, the bimolecular equilibrium which appears to be operative in the present system at low temperatures is the one leading to ion pair formation (eq 5).

Anisotropic Broadening. The ESR spectra of Rh(dppe)$_2^0$ are further complicated by an increase in the viscosity of the toluene as the temperature decreases. This leads to a slowing of the molecular tumbling in solution and an unsymmetrical broadening of the ESR lines due to incomplete averaging of anisotropies in the **g** and hyperfine tensors.[17,18] The effect is readily seen in Figure 1 and is more pronounced at the lowest temperatures. The observed broadening is dependent on the nuclear spin quantum numbers of the transitions and is in general expressable as a power series in the nuclear spin quantum numbers.[3,18,19] For the present system containing two sets of completely equivalent P nuclei, the anisotropic broadening can be accommodated by using eq 10. In

$$\text{width} = \alpha_0 + \beta_1 M_1 + \beta_2 M_2 + \gamma_1 M_1^2 + \gamma_2 m_2^2 + (\epsilon_{12} + \epsilon_{21}) M_1 M_2 \quad (10)$$

this equation, M_i is the nuclear spin quantum number for the ith set of completely equivalent P nuclei with $M_i = m_{i1} + m_{i2}$. The paramter α_0 is the residual line width including the broadening due to the alternating line width effect, while β_i is related to both the **g** and hyperfine anisotropies, and γ_i and ϵ_{ij} are parameters related only to anisotropies in the hyperfine tensors. All of these quantities are directly proportional to the rotational correlation time.[3,18,19]

The calculated spectra in Figure 2 take into account anisotropic broadening using eq 10 with values for the parameters adjusted to give good visual agreement between the observed and calculated spectra. While variation of these parameters affected line shapes in the calculated spectra, they did not alter the positions of the observed lines. Because of the number of adjustable parameters, no attempt was made to refine them by a mathematically rigorous procedure. Values of α_0, β_i, γ_i, and ϵ_{ij} are given in a footnote.[20]

Table II. ESR Intensities and Equilibrium Constants at Different Temperatures[a]

T (K)	I^T	α	10^2 K (M^{-1})
249	25935		
237	23641	0.868	0.219
229	20235	0.718	0.683
219	11549	0.392	4.94
209	6702	0.217	20.78
199	4220	0.130	64.35
189	2099	0.061	315.4

[a] I^T is the integrated intensity of the ESR absorption spectrum expressed in arbitrary units at temperature T; α is the fraction of Rh(dppe)$_2$ species present as the paramagnetic monomer calculated by using eq 8; and K is the equilibrium constant calculated with eq 6.

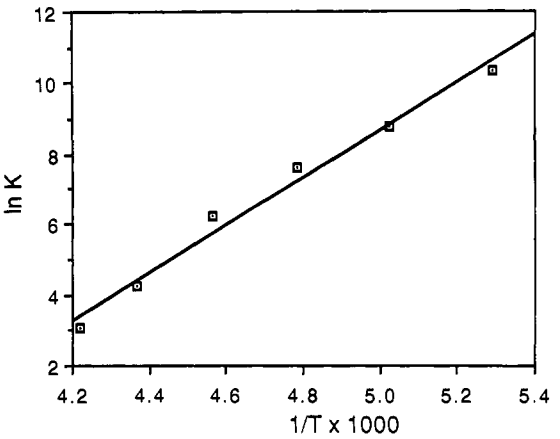

Figure 4. Van't Hoff plot of the bimolecular equilibrium involving Rh(dppe)$_2^0$.

Reaction of Rh(dppe)$_2^0$ with Molecular Hydrogen. Previously we reported that Rh(dppe)$_2^0$ is relatively unreactive with certain protic and H-atom sources.[7] Indeed, blue solutions of Rh(dppe)$_2^0$ in benzene were observed to maintain their color in the presence of MeOH, MeCN, cumene, and Ph_3CH for hours at room temperature. Despite this apparent lack of reactivity, Rh(dppe)$_2^0$ in benzene reacts with molecular hydrogen over a period of several hours to form the hydride complex RhH(dppe)$_2$ quantitatively, eq 11, as determined by ^{1}H NMR spectroscopy.

$$2Rh(dppe)_2^0 + H_2 \rightarrow 2RhH(dppe)_2 \quad (11)$$

The occurrence of eq 11 is a relatively rare example of H_2 activation by odd-electron complexes yielding monohydride products. Among previous examples is eq 12 involving the well-studied $Co(CN)_5^{3-}$ system.[21,22] Equation 12 proceeds by a

$$2Co(CN)_5^{3-} + H_2 \rightarrow 2CoH(CN)_5^{3-} \quad (12)$$

rate law that is second order in complex and first order in H_2 and a mechanism involving a pre-equilibrium step.[23] Recently, Nixon has examined the reaction chemistry of Rh(P(O-*i*-Pr)$_3$)$_4^0$ and has observed a similar reactivity with H_2.[12] Other examples of H_2 activation by odd-electron Rh complexes or their related dimers include the reversible reaction of [Rh(OEP)]$_2$ (OEP = octa-

(17) Carrington, A.; McLachlan, A. D. *Introduction to Magnetic Resonance*; Harper and Row: New York, 1967; pp 197–199.
(18) (a) Wilson, R.; Kivelson, D. *J. Chem. Phys.* **1966**, *44*, 154. (b) Fraenkel, G. K. *J. Phys. Chem.* **1967**, *71*, 139.
(19) Peake, B. M.; Rieger, P. H.; Robinson, B. H.; Simpson, J. *Inorg. Chem.* **1979**, *18*, 1000.

(20) The values for the parameters in the anisotropic line broadening correction given by eq 10 are

temp (K)	α_0	β_1	β_2	γ_1	γ_2	$(\epsilon^{12} + \epsilon^{21})$
259	4	−0.5	−0.5	−0.5	−0.5	3.0
249	4	−0.5	−0.5	−0.5	−0.5	3.0
237	4	−0.5	−0.5	−0.5	−0.5	3.0
219	5	−0.5	−0.5	−0.5	−0.5	3.0
209	5	−0.5	−0.5	−0.5	−0.5	2.0
199	7.5	−0.9	−2.0	−0.25	0.5	2.2

The spectrum at 199 K was simulated by using a local least-squares program written in ASYST.
(21) James, B. R. *Homogeneous Hydrogenation*; Wiley-Interscience: New York, 1973; Chapter 10 and references therein.
(22) DeVries, B. *J. Catal.* **1962**, *1*, 489.
(23) Halpern, J.; Pribanic, M. *Inorg. Chem.* **1970**, *9*, 2616.

ethylporphyrin) with H_2, eq 13,[24] and the equilibrium shown as (14) involving the hydroformylation catalyst $RhH(CO)_2(PPh_3)_2$ and a related Rh(0) dimer.[25] Recent studies indicate that the mechanism for (13) proceeds via an odd-electron Rh(II) monomer.[26]

$$Rh_2(OEP)_2 + H_2 \rightleftharpoons 2RhH(OEP) \quad (13)$$

$$2RhH(CO)_2(PPh_3)_2 \rightleftharpoons Rh_2(\mu\text{-}CO)_2(CO)_2(PPh_3)_2 + H_2 \quad (14)$$

Because of the unusual nature of eq 11, the kinetics and mechanism of the reaction will be investigated further.

Experimental Section

Benzene was distilled from dark purple solutions of sodium benzophenone ketyl under vacuum, and toluene was distilled from CaH_2 under vacuum. The complex $[Rh(dppe)_2](BF_4)$ was prepared by literature procedures.[7]

ESR Measurements. Samples of $Rh(dppe)_2^0$ were prepared by reduction of $Rh(dppe)_2^+$ with sodium naphthalenide in THF as described previously.[7] ESR spectra were recorded at 9.65 GHz on a Bruker ER 200 D spectrometer fitted with a liquid nitrogen flow system and heater/controller for obtaining temperatures down to that of liquid nitrogen.

Spectra were calculated by using a locally modified version of the program EALTW written by Sullivan and Bolton. The local modification incorporates anisotropic broadening as described in the text.

Reaction of $Rh(dppe)_2^0$ with H_2. A blue solution of $Rh(dppe)_2^0$ in benzene-d_6 was placed in an NMR tube, which was connected to a vacuum line and sealed under 500 Torr of H_2. The reaction was followed over a 5-h period by ^1H NMR spectroscopy. The product was identified by comparison with an authentic sample of $RhH(dppe)_2$ prepared independently by reported procedures.

Acknowledgment. We thank the National Science Foundation (CHE 83-08064 and 86-05033) for support of this work and the Johnson Matthey Co., Inc. for a generous loan of rhodium salts. We also acknowledge helpful discussions with Dr. Paul Krusic and Dr. Tom Baker of DuPont and Professor Philip Rieger of Brown University.

(24) Wayland, B. B.; Woods, B. A.; Pierce, R. *J. Am. Chem. Soc.* **1982**, *104*, 302.
(25) Evans, D.; Yagupsky, G.; Wilkinson, G. *J. Chem. Soc., Sect. A* **1968**, 2660. Yagupsky, M.; Brown, C. K.; Yagupsky, G.; Wilkinson, G. *J. Chem. Soc., Sect. A* **1970**, 937.
(26) Paonessa, R. S.; Thomas, N. C.; Halpern, J. *J. Am. Chem. Soc.* **1985**, *107*, 4333.

Tetranuclear Iron–Oxo Complexes. Synthesis, Structure, and Properties of Species Containing the Nonplanar $\{Fe_4O_2\}^{8+}$ Core and Seven Bridging Carboxylate Ligands

William H. Armstrong, Mary E. Roth, and Stephen J. Lippard*

Contribution from the Department of Chemistry, Massachusetts Institute of Technology, Cambridge, Massachusetts 02139. *Received March 23, 1987*

Abstract: The synthesis and structure of the novel tetranuclear complexes $[Fe_4O_2(O_2CR)_7(H_2B(pz)_2)_2]^-$, where R = Me or Ph and $H_2B(pz)_2^-$ = dihydrobis(1-pyrazolyl)borate, are described. These complexes may be viewed formally as the 2 + 2 condensation products of two $\{Fe_2O(O_2CR)_2\}^{2+}$ cores, containing iron atom pairs Fe_AFe_B and Fe_CFe_D, to form $\{Fe_4O_2(O_2CR)_4\}^{4+}$, in which both of the oxo ligands are triply bridging. A four-membered Fe_2O_2 unit, comprised of iron atoms Fe_B and Fe_C, at the center of the tetranuclear complex is bridged by a single benzoate group, and two additional singly bridging benzoate groups link the remaining iron atom pairs, Fe_AFe_C and Fe_BFe_D. In the structure of $(Et_4N)[Fe_4O_2(O_2CPh)_7(H_2B(pz)_2)_2]$, the Fe–O ($\mu_3$-oxo) distances within the $\{Fe_2O(O_2CPh)_2\}^{2+}$ units are 1.822 (7) and 1.854 (8) Å for bonds to Fe_A and Fe_D and 1.895 (7) and 1.917 (7) Å for bonds to Fe_B and Fe_C. The Fe–O (μ_3-oxo) bonds linking these halves of the tetranuclear aggregate are 1.955 (8) and 1.967 (8) Å. The $\{Fe_4O_2\}^{8+}$ core is distorted from planarity, presumably by the additional bridging carboxylate ligands, with deviations of ±0.5 Å or less from the best plane through the four iron atoms. The deviation of Fe_A or Fe_D from the plane defined by the other three iron atoms is 1.8 Å. Proton nuclear magnetic resonance studies of $[Fe_4O_2(O_2CR)_7(H_2B(pz)_2)_2]^-$ complexes, dissolved in CD_2Cl_2, are consistent with the X-ray structural results. Solution-state magnetic susceptibility data also confirm the integrity of the $\{Fe_4O_2\}^{8+}$ core. The optical spectrum of $[Fe_4O_2(O_2CR)_7(H_2B(pz)_2)_2]^-$ in solution is similar to, but distinct from, that of the binuclear analogues $[Fe_2O(O_2CR)_2(HB(pz)_3)_2]$. A Raman band at 746 cm^{-1} was identified as being characteristic of the $\{Fe_4O_2\}^{8+}$ core. Magnetic susceptibility measurements reveal a diamagnetic ground state with antiferromagnetic exchange interactions among the four high-spin ferric centers. Zero-field Mössbauer spectra at four temperatures display a single quadrupole doublet with an isomer shift of 0.52 mm/s, consistent with high-spin Fe(III). The relevance of this chemistry to the synthesis of functional models for the oxo-bridged binuclear iron cores of hemerythrin and related proteins is discussed.

The diiron cores of the marine invertebrate respiratory protein hemerythrin (Hr)[1] and related proteins including ribonucleotide reductase (RR)[2] and the purple acid phosphatases[3] have been the subject of recent modeling studies by bioinorganic chemists.[4-6] Binuclear iron(III) complexes containing both oxo and carboxylato bridging ligands have been synthesized and shown to be excellent spectroscopic and magnetic models for Hr and RR.[4-6] Reactivity studies of the $\{Fe_2O(O_2CR)_2\}^{2+}$ core have further aided our un-

(1) (a) Wilkins, R. G.; Harrington, P. C. *Adv. Inorg. Biochem.* **1983**, *5*, 51–85. (b) Harrington, P. C.; Wilkins, R. G. *Coord. Chem. Rev.* **1987**, *79*, 195–214.
(2) (a) Sjöberg, B.-M.; Gräslund, A. *Adv. Inorg. Biochem.* **1983**, *5*, 87–110. (b) Lammers, M.; Follman, H. *Struct. Bonding (Berlin)* **1983**, *54*, 27–91.
(3) Antanaitis, B. C.; Aisen, P. *Adv. Inorg. Biochem.* **1983**, *5*, 111–136.
(4) (a) Armstrong, W. H.; Lippard, S. J. *J. Am. Chem. Soc.* **1983**, *105*, 4837–4838. (b) Armstrong, W. H.; Spool, A.; Papaefthymiou, G. C.; Frankel, R. B.; Lippard, S. J. *J. Am. Chem. Soc.* **1984**, *106*, 3653–3667.
(5) Wieghardt, K.; Pohl, K.; Gebert, W. *Angew. Chem., Int. Ed. Engl.* **1983**, *22*, 727.
(6) Toftlund, H.; Murray, K. S.; Zwack, P. R.; Taylor, L. F.; Anderson, O. P. *J. Chem. Soc., Chem. Commun.* **1986**, 191–193.

0002-7863/87/1509-6318$01.50/0